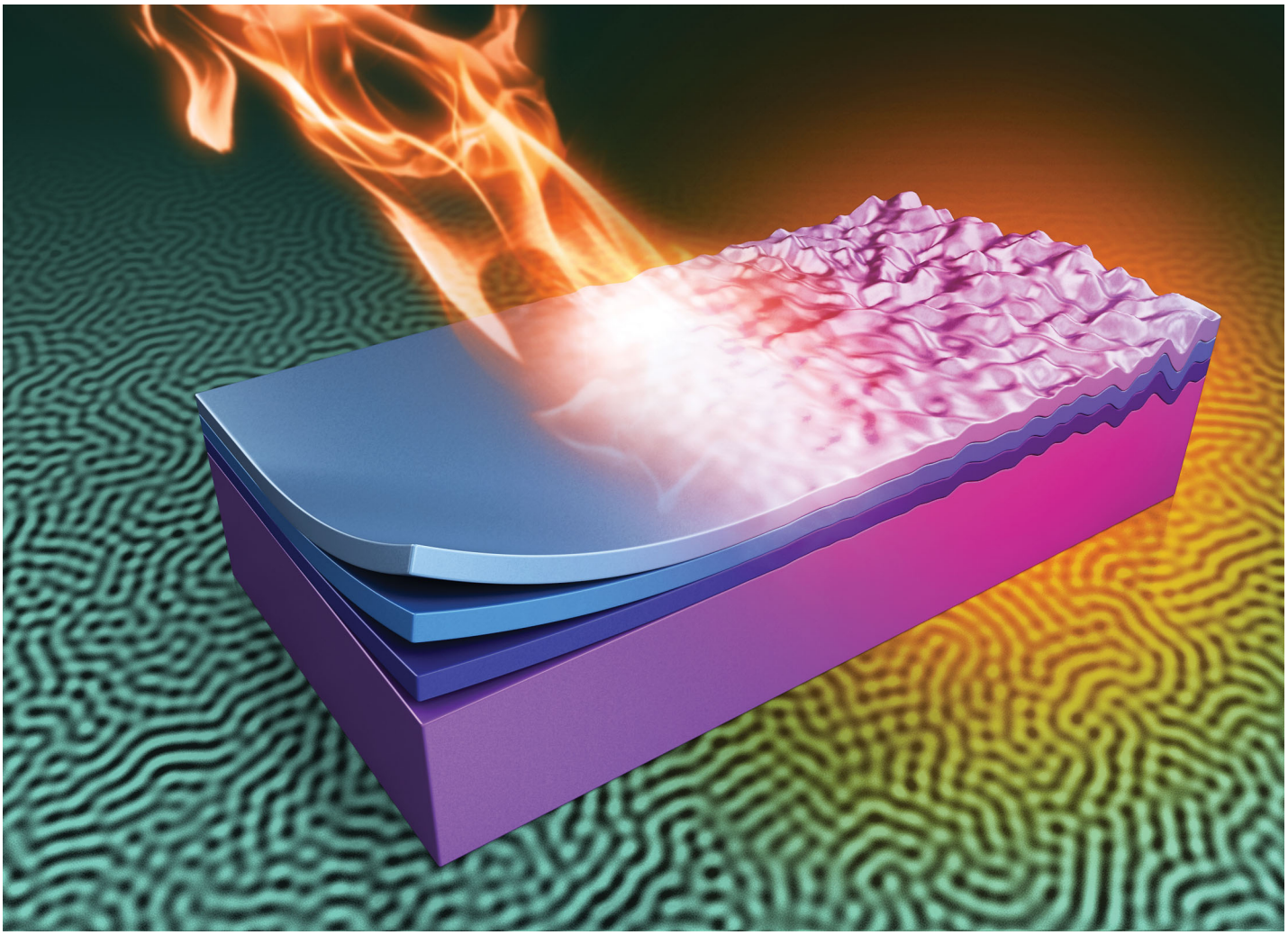

Highlighting research from Sungkyunkwan University (SKKU) from the group of Prof. Pil J. Yoo.

Cumulative energy analysis of thermally-induced surface wrinkling of heterogeneously multilayered thin films

Tri- or quad-layer systems of polymer/metal multilayers are thermally treated to generate surface wrinkles, which is interpreted with cumulative energy balance analysis to consider the individual elastic contribution of each constituent layer. Unlike the conventional composite layer model, the presented approach precisely reflects the bending energy contribution of the given multilayer system, suggesting a powerful toolkit for creating controlled surface wrinkles with the targeted wavelength.

As featured in:

See Pil J. Yoo *et al.*, *Soft Matter*, 2018, **14**, 704.

ROYAL SOCIETY OF CHEMISTRY

rsc.li/soft-matter-journal

Registered charity number: 207890

Soft Matter

PAPER

View Article Online
View Journal | View Issue

Cite this: *Soft Matter*, 2018, **14**, 704

Cumulative energy analysis of thermally-induced surface wrinkling of heterogeneously multilayered thin films†

Seong Soo Yoo,[a] Gwan H. Choi,[a] Wooseop Lee,[b] Juhyun Park,[c] Gi-Ra Yi,[a] Du Yeol Ryu[b] and Pil J. Yoo*[ad]

Received 12th October 2017,
Accepted 15th December 2017

DOI: 10.1039/c7sm02027a

rsc.li/soft-matter-journal

Wrinkling is a well-known example of instability-driven surface deformation that occurs when the accumulated compressive stress exceeds the critical value in multilayered systems. A number of studies have investigated the instability conditions and the corresponding mechanisms of wrinkling deformation. Force balance analysis of bilayer systems, in which the thickness of the capping layer is importantly considered, has offered a useful approach for the quantitative understanding of wrinkling. However, it is inappropriate for multilayer wrinkling (layer number > 3) consisting of heterogeneous materials (*e.g.* polymer/metal or inorganic), in which the thickness variation in the substrate is also crucial. Therefore, to accommodate the additive characteristics of multilayered systems, we thermally treated tri- or quad-layer samples of polymer/metal multilayers to generate surface wrinkles and used a cumulative energy balance analysis to consider the individual contribution of each constituent layer. Unlike the composite layer model, wherein the thickness effect of the capping layer is highly overestimated for heterogenously stacked multilayers, our approach precisely reflects the bending energy contribution of the given multilayer system, with results that match well with experimental values. Furthermore, we demonstrate the feasibility of this approach as a metrological tool for simple and straightforward estimation of the thermomechanical properties of polymers, whereby a delicate change in the Young's modulus of a thin polymeric layer near its glass transition temperature can be successfully monitored.

Introduction

Surface wrinkling is a spontaneous phenomenon that occurs in multilayered thin films when the accumulated compressive stress exceeds the threshold magnitude, the critical wrinkling stress.[1] To induce compressive stress, various driving forces have been used, such as mechanical compression,[2–4] thermal annealing,[5,6] and solvent-induced swelling.[7,8] Whereas traditional studies on wrinkling focused on physically interpreting thin films under instability in order to circumvent undesirable deformation of the system, recent works have aimed to direct the surface wrinkling in a pre-determined way to form unconventional wavy patterns with specific optical characteristics or surface properties.[9–11] In addition, a wrinkling-based metrology has been developed to estimate the mechanical properties of an unknown thin layer by simply measuring the size or evolutional behaviours of surface wrinkles.[12,13] Due to its versatility with various types of materials and a wide range of thin film thicknesses (from several nm to tens of μm), this metrology has been broadly used to estimate the elastic modulus of thin films in organic electronics,[14] solar cells,[15] and nanocomposites.[16]

Analyses of surface wrinkling instability have focused mostly on simple bilayer systems: *i.e.*, a single thin layer placed on a deformable semi-infinite-thick soft substrate[17–19] or a bilayer thin film on a non-deformable rigid support.[20–22] Despite its greater relevance to currently developed multilayered optic systems, optoelectronics, and wearable devices, which include complexly layered thin films of heterogenous materials,[23] the wrinkling of multilayered films composed of more than three layers (*e.g.*, tri-layer or quad-layer) has been rarely studied (in this study, heterogeneous multilayered films refer to systems containing more than three thin layers comprising materials with a large difference in their elastic properties). Improved controllability of

[a] *School of Chemical Engineering, Sungkyunkwan University (SKKU), Suwon 16419, Republic of Korea. E-mail: pjyoo@skku.edu*
[b] *Department of Chemical and Biomolecular Engineering, Yonsei University, Seoul 03722, Republic of Korea*
[c] *School of Chemical Engineering and Materials Science, Chung-Ang University, Seoul 06974, Republic of Korea*
[d] *SKKU Advanced Institute of Nanotechnology (SAINT), Sungkyunkwan University (SKKU), Suwon 16419, Republic of Korea*

† Electronic supplementary information (ESI) available. See DOI: 10.1039/c7sm02027a

multilayered films requires the elaboration of surface wrinkling phenomena and a more comprehensive interpretation of the wrinkling mechanism and corresponding instability.

Previous works on the wrinkling instability of bilayer systems have been based on a force balance analysis using the classical bending equation for thin films, which describes the competition between a bending force in the coating layer and the loading force of the underlying substrate.[24,25] When the condition of force minimization is attained, the bilayer system exhibits surface wrinkling with a characteristic wavelength.[26] In the case of multilayer wrinkling, the number of bending layers atop the substrate increases, requiring a modified or alternative force balance equation to interpret the corresponding system. To simplify the system and make it similar to the conventional bilayer model, the multiple bending layers on the substrate are regarded as a single composite layer with an intermediate value for the elastic properties.[27] Such a composite model explains well the deformation behavior of multilayers consisting of elastically similar materials since the resulting multilayer film is almost close to a homogeneously mixed system. Recently, a more complex numerical approach considered the multilayers as an integration of individual layers. That model independently considers the modulus, moment of inertia, and stiffness values of the constituting layers to provide more accurate properties for the resulting surface wrinkles.[28]

It should be noted that substrate deformation by the loading force is reflected by the undulation of the wrinkling waves, and the effect of the substrate thickness is generally not considered in the force balance analysis.[24–26] Applying this condition to a system is experimentally valid when the thin film is placed on a semi-infinitely-thick soft substrate. However, when a bilayer or multilayer thin film is placed on a non-deformable rigid support, the compressive stress for wrinkling is generated by the difference between the expansion coefficients of the constituting layers; a relevant example can be found in metallic capping, in which underlying polymeric layers are coated onto a rigid Si support.[29] The intermediate layer (polymer) is confined between the capping layer (metal) and the support (Si), so it works as the substrate medium for deformation, and the effect of its thickness variation is salient in determining the wrinkling characteristics. Therefore, the governing equation for wrinkling needs to be modified to reflect the thickness effect of the constituting layer.

The energy balance approach is another way to describe surface wrinkling that reaches the moment of thermodynamic equilibrium.[30,31] Similar to the force balance analysis, the energy balance equation for bilayer wrinkling considers the bending energy term of the capping layer and the deformation energy term for the underlying substrate.[32] Notably, because it can independently consider the contribution from thickness variations in both layers, the energy balance analysis has been widely used to interpret wrinkling in thin bilayers on a rigid support.[33,34] Specifically, the bending energy term assumes homogeneous bending deformation of the capping layer with a constant strain tensor throughout the film.[35] Therefore, a multilayered capping layer is generally treated as a single and homogeneous composite layer, with the average value used for the elastic properties. This assumption appropriately applies to a multilayered system comprising similar materials, such as polymer/polymer or metal/inorganic systems. However, because the bending energy is proportional to the cube of the capping layer thickness,[36] the composite model approximation results in a severe overestimation of the capping layer's bending energy contribution to the overall surface wrinkling (mathematical details are discussed below), especially for the multilayered systems comprising elastically heterogeneous materials (*e.g.* polymer/metal or inorganic). Therefore, special attention is required to interpret heterogeneous multilayer wrinkling using the energy balance analysis. The bending deformation of the constituent capping layers should be considered individually, rather than through the composite layer model.

In this work, to accommodate the complexity of bending deformation in the capping layers, we used an individual layer model to reflect the cumulative contribution of each capping layer to the surface wrinkling of thin multilayered films with heterogeneous materials. Typically, a multilayered system consists of hard capping layers (multiple stacks of metal and polymeric thin layers) for upper bending and polymeric substrates for underlying undulating deformation, all on top of a rigid Si support. When the temperature is raised above the glass transition temperature (T_g) of the polymeric substrate, an abrupt reduction in the Young's modulus and a subsequent increase in the thermal expansion coefficient inside the polymeric layer generate a large amount of compressive stress, which causes surface wrinkling.[37] Because the capping layer is composed of heterogeneous stacks of multiple thin layers, the bending energy for each layer can be counted independently in order to obtain the optimum wrinkling wavelength under a minimized energy condition. The wrinkling wavelength estimated by our model matched the experimental results for tri- and quad-layer systems more accurately than the wavelengths obtained from the traditional bilayer composite model. In addition, to demonstrate our approach's feasibility as a metrological tool, we investigated multilayer wrinkling by including the polymeric capping layer and obtained a highly reasonable trend in the change of Young's modulus near the glass transition temperature according to temperature variations. Therefore, our approach will expand the applicability of wrinkling-based metrology to complex heterogeneously multilayered systems.

Experimental

Preparation of multilayered films

Tri-layer films used a polystyrene (PS) layer as the substrate and Al and poly(4-vinylpiridine) (PVP) layers as the capping film. All layers were placed on a Si wafer support. To prepare tri-layer films, the Si wafer was cleaned by ultrasonic treatment for 5 min in each of acetone, ethanol, and water and then dried in nitrogen gas. The native oxide was not removed from the surface. The first PS layer (M_n 1 050 000, M_w/M_n = 1.09, $T_{g,bulk} \approx 105$ °C, Polymer Source Inc.) was spin coated with a toluene solution onto a

Si wafer to the target thickness by varying the solution concentration or the spin-coating speed. The samples were annealed at 60 °C for 12 h to remove the residual solvent and relieve the stress caused by the spin coating. For the second layer, Al was deposited onto the prepared PS surface to the desired thickness by thermal evaporation under high vacuum (5×10^{-6} Torr) with a deposition rate of 5–10 Å s^{-1}. To prevent the thermal memory effect in the underlying PS layer, the samples were loaded far (~60 cm) from the crucible at a relatively fast deposition rate. For the third layer, P4VP (M_n 160 000, $T_{g,bulk} \approx 142$ °C, Sigma Aldrich) was used, and a solution in butanol was spin coated onto the Al–PS bilayer surface. Finally, the tri-layer samples were annealed at 70 °C for 24 h to completely remove the residual solvent. To prepare quad-layer samples, an additional Al layer was thermally deposited onto the prepared tri-layer, resulting in PS–Al–P4VP–Al layered films.

Generation of surface wrinkles

In this study, surface wrinkling was induced using thermal stress by annealing. Multilayer samples were heated to 140 °C, which is higher than T_g of PS (the substrate layer) and lower than T_g of P4VP, so that the tendency of lateral expansion in the softened PS layer could generate compressive stress for wrinkling while stably allowing for bending deformation in the elastically responsive capping layer made of Al and P4VP. To ensure enough time above T_g for chain rearrangement in the softened PS layer, the annealing temperature was maintained for 12 h.

Characterization

The wrinkled surface was investigated using an atomic force microscope (AFM, Dimension 3100, Veeco, US) in tapping mode under dry conditions. To minimize any possible errors during data acquisition and to enhance image resolution, we used tapping mode at a slow scanning rate (scan speed of 0.3–0.5 Hz). The characteristic wavelength of the surface wrinkles was calculated using the AFM software provided by Veeco (version 5.31r1). The glass transition temperature of thin polymeric films was measured on a lab-made heating stage using spectroscopic ellipsometry (SEMG-1000, Nanoview Co.) inside the vacuum chamber. The ellipsometer was operated at an incidence angle of 70° with a halogen light source at wavelengths (λ) ranging from 350 to 850 nm. For accurate measurements of the film thickness variation below 100 nm, a UV-vis light source was also used to cover wavelengths ranging from 250 to 850 nm where a deuterium–tungsten lamp (Hamamatsu Photonics, Japan) was used as the light source. Among the two ellipsometric angles related to the film thickness (Ψ and δ), Ψ was measured continuously as the temperature increased from 30 to 200 °C at a heating rate of 2 °C min^{-1}. The obtained values of Ψ changed as the temperature increased. In particular, Ψ started to increase or decrease sharply at the glass transition temperature of the polymeric film.

Results and discussion

As discussed in the Introduction, energy balance analysis is based on the competition between the bending free energy of the capping layer, which tends to have a larger wavelength, and the deformation free energy of the substrate, which tends to have a smaller wavelength. For heterogeneously multilayered film systems that include multiple capping layers (schematically depicted in Fig. 1a), conventional approaches have regarded the stacked capping layers as a homogeneous composite film (Fig. 1b) to meet the needs of the bilayer model.[27,38] However, in this study, we consider the accumulated bending energy contributed by each layer to derive an individual layer model. When a multilayer system consists of a single underlying deformation layer and 'n' bending capping layers, the extended free energy expression for the multilayered system can be given by[32]

$$F = \left(\sum_{c=1}^{n} \frac{E_c t_c^3}{48(1-\nu_c^2)} \varepsilon^2 k^4 \right)_{\text{bending}} + \left(\frac{E_s \varepsilon^2}{4k^2 t_s^3} + \frac{1}{6} E_s \varepsilon^2 k \right)_{\text{deformation}} \quad (1)$$

where E is the Young's modulus of the layer, t is the thickness of the layer, and ε is the amplitude of the wrinkling wave. The wavelength λ is $2\pi/k$, where k is the wave number, and ν is Poisson's ratio of the layer. The subscripts c and s represent the capping layer and substrate layer, respectively. Because the surface wrinkles do not include delamination or interfacial separation between the capping and substrate layers, the bending deformations in multiple capping layers are expected to be identical in amplitude and wave number. This assumption is valid for the current multilayered system comprising PS, P4VP, and Al layers, because a metallic Al layer is known to have strong adhesion with polymers. However, if a non-interfacial-affinitive metallic layer is employed (*e.g.* Au), an interfacial slip between the metal and the polymer would occur and the surface wrinkling behavior needs to be interpreted with a kinetic model.

It is generally observed that the lateral wavelength of surface wrinkles is much greater than the layer thickness and wrinkling amplitude in the longitudinal direction, *i.e.*, shallow undulations. It should also be noted that eqn (1) is valid for the heterogeneously multilayered system in which elastically different materials are layered, such that the bending deformations of each capping layer are individually separated. By contrast, when elastically similar materials are stacked, the upper phase of multilayers is rather regarded as a single composite

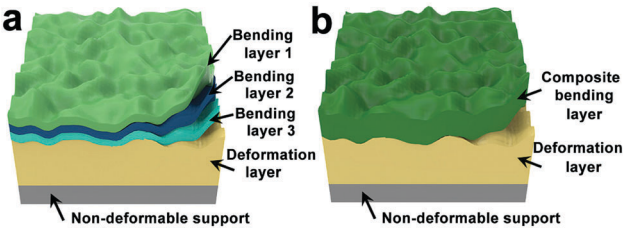

Fig. 1 Schematic illustration of the multilayered film system considered in this study. (a) The quad-layer films consist of three bending layers and an underlying deformation layer that are individually stacked on a non-deformable rigid support. (b) Conventionally, this multilayer model is simplified into a bilayer model in which the multiple bending layers are considered as a single composite layer.

capping layer and the system needs to be interpreted with a traditional bilayer model. Therefore, the cumulative approach presented in eqn (1) can be plausibly accepted for the experimental system proposed in this study. When the free energy of the heterogeneously multilayered system shown in eqn (1) is minimized with respect to the wave number, the optimum wavelength of the surface wrinkles can be estimated as follows.

$$\lambda_{\text{individual}} = 2\pi \left(\frac{-1 + \sqrt{1 + 6\left(\sum_{c=1}^{n} \frac{E_c t_c^3}{1 - v_c^2}\right)\frac{1}{E_s t_s^3}}}{\frac{1}{E_s}\left(\sum_{i=1}^{n} \frac{E_c t_c^3}{1 - v_c^2}\right)} \right)^{-\frac{1}{3}} \quad (2)$$

To evaluate the validity of the estimated wrinkling wavelength proposed in eqn (2), we compared the calculated values with experimental results. As explained in the Experimental section, the heterogeneous multilayered film system used here includes two polymeric layers: PS as the substrate and P4VP as one of the capping layers. We chose these two polymers for two reasons: (1) they are not compatible in a co-solvent; thus, it is possible to carry out spin-coating of PS and P4VP sequentially without concern about deteriorating the pre-coated layer, and (2) T_g of P4VP is greater than that of PS, which enables the P4VP layer to remain as a glassy capping layer at the elevated annealing temperature (140 °C). In the experiments, tri-layer (PS of 400–720 nm, Al of 13 nm, and P4VP of 20 nm) and quad-layer (PS of 400–650 nm, Al of 15 nm, P4VP of 20 nm, and Al of 15 nm) samples were used. Surface wrinkles were generated when the samples were heated above T_g of PS, and the thermally induced compressive stress exceeded the critical threshold for wrinkling.

Experimental results for tri-layer wrinkling with PS substrates of various thicknesses are presented in Fig. 2a. In accordance with the general theory for thermal wrinkling of metal/polymer multilayered films, the wrinkling wavelength gradually increases with the thickness of the underlying PS substrate layer. The trend of wrinkling wavelength estimated using eqn (2) was compared with the measured wavelengths using fast Fourier transform (FFT) analysis and is presented in Fig. 2b (tri-layer) and Fig. 2c (quad-layer). Here, the following parameters were used to obtain the theoretical values: E_{P4VP} of 4 GPa,[39] E_{Al} of 70 GPa, and Poisson's ratio of 0.33 for both Al and P4VP. Because the annealing temperature of 140 °C is higher than T_g of PS (105 °C), the E_{PS} value needs to be modified to reflect the loosely disentangled behaviour of the PS chains. Since the annealing temperature is much lower than the flowing temperature of PS, the PS film annealed at 140 °C is expected to exhibit mostly elastic thermomechanical behaviour while suppressing a consideration for viscoelasticity. The elastic properties of a thermoplastic polymer above its glass transition temperature are known to follow the mathematical relationship of the Williams–Landel–Ferry (WLF) equation:[32,40]

$$E_{\text{PS}} = E_{\text{PS},0} \exp\left(\frac{-C_1(T - T_r)}{C_2 + T - T_r}\right) \quad (3)$$

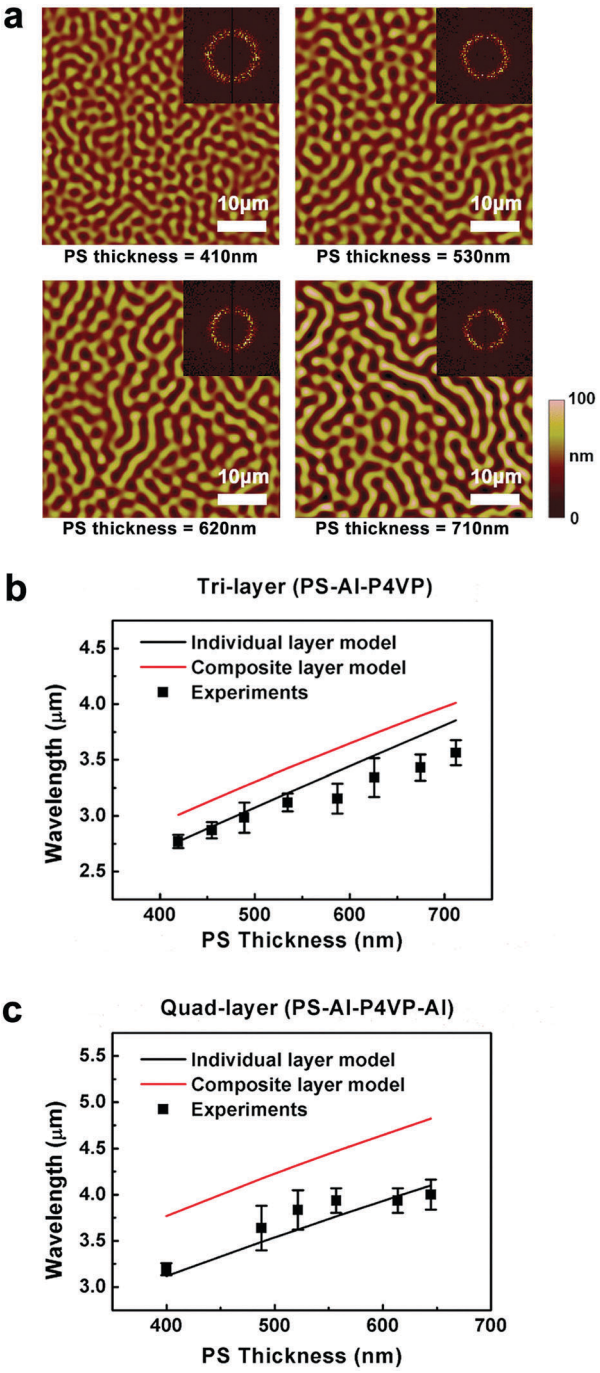

Fig. 2 (a) AFM images of surface wrinkles developed in tri-layer (PS–Al–P4VP) films with various thicknesses of PS substrates (scan size = 50 μm × 50 μm). Comparison between the theoretical estimations (solid lines) and experimental results (square dots) for (b) tri-layer and (c) quad-layer systems. Error bars represent the standard deviation.

where $E_{\text{PS},0}$ is E_{PS} at a reference temperature of T_r, which is often taken as the glass transition temperature, and C_1 and C_2 are the constants unique to a given material. For the system being considered, T_r = 378 K, C_1 = 9.87, C_2 = 47.3 K,[41] and $E_{\text{PS},0}$ = 3.2 GPa. Because P4VP in the capping layer is very thin (20 nm), T_g of P4VP may vary through its interactions with the

underlying layer or the confinement effect.[42,43] Typically, the strong affinity between the underlying Al layer and P4VP thin film[44] increases T_g above that of bulk phase P4VP (142 °C).[45] To obtain the effective value of T_g for the ultrathin P4VP layer, we used ellipsometric measurements and obtained a T_g of 148 °C for P4VP (see ESI,† S1). Therefore, under the thermal annealing condition at 140 °C, the P4VP layer in the capping layer would retain its glassy and elastic properties.

The solid lines in Fig. 2b and c show the plots of the estimated wrinkling wavelength on the basis of the traditional composite layer model (red) and our individual layer model (black) for the capping layer. The individual layer model achieves good agreement with the experimental values, whereas the composite layer model overestimates the wavelengths by ~10% compared with the experimental results. The composite layer model needs to consider the effective value of Young's modulus for the homogeneous composite layer, which can be derived from the standard plate mechanics for a bilayer system.[46]

$$E_{\text{eff}} = \frac{1 + m^2n^4 + 2mn(2n^2 + 3n + 2)}{(1+n)^3(1+mn)}E_{\text{lower}} \qquad (4)$$

where m is the modulus ratio of $E_{\text{upper}}/E_{\text{lower}}$, and n is the thickness ratio of $t_{\text{upper}}/t_{\text{lower}}$. Accordingly, in eqn (1), t_c is the combined thickness of the upper and lower layers in the capping film. Because eqn (4) is valid for bilayer composite systems, *i.e.*, tri-layer for wrinkling, the effective modulus for tri-layered composite films (quad-layer for wrinkling) should be obtainable in an iterative way using eqn (4).

Considerably large deviations between the composite layer model and the experimental data can be ascribed to the overestimated bending energy of eqn (1), in which $F_{\text{bending}} \sim E_c t_c^{\,3}$. Because the estimated effective modulus from standard plate mechanics is known to be highly relevant to actual multilayered systems,[12,27] the overestimation in bending energy originates mainly from the thickness term. In deriving the mathematical expression for bending free energy, the strain tensor generated from the homogeneous composite body is assumed to be uniform (see ESI,† S2).[35,36] As shown in the derivation process, the bending energy for a controlled volume is proportional to the square of the strain tensor, which is proportional to the film thickness. Also, because the total bending energy for a body is integrated from the controlled volume energy, the overall bending free energy is accordingly proportional to the cube of the film thickness. Therefore, despite the methodological accuracy in estimating the effective modulus value from standard plate mechanics, the contribution from the combined thickness would significantly affect the increase in bending free energy in the composite layer model. An increase in bending energy indicates the tendency for a larger wavelength in wrinkling. However, this expected condition in the composite layer model excludes the presence of the underlying substrate layer, which tends toward a small deformation (smaller wavelength). Therefore, the estimated wavelengths from the composite model are consequently larger than the actual experimental values. It needs to be noted that this deviation between experimental and theoretical estimation for the composite model would decrease and be negligibly small when the multilayered systems are prepared with similar materials (*i.e.* homogeneous multilayers).

Another way to consider the above discussed idea would be to harness them to effectively reduce the wavelength of surface wrinkles, even under identical geometric conditions: given a particular capping layer thickness, a multilayer-stacked system would generate smaller wrinkles than a system with fewer layers. For example, in a tri-layer system with PS (490 nm)/Al (20 nm)/P4VP (20 nm) and a quad-layer system with PS (490 nm)/Al (10 nm)/P4VP (20 nm)/Al (10 nm), the total thickness and overall composition are identical. However, according to the approach presented above, the wrinkling wavelength from the quad-layer system will be smaller than that from the tri-layer system because the bending free energy exhibits a thickness dependence on third-order kinetics. As shown in Fig. 3a, the experimentally observed wavelength from the quad-layer system matches our expectation: it is smaller than that from the tri-layer system. The trend of wavelength reduction in multilayer systems is also summarized in Fig. 3b. Clearly, the distribution of bending energy into multiple stacks of capping layers efficiently reduces the total amount of bending free energy, resulting in a reduction in the wrinkling wavelength. This could be very beneficial for creating a structure with fine wrinkles, which is important in unconventional patterning and optical applications responsive to light with a specific wavelength.[47,48]

Finally, the approach to cumulative energy analysis suggested in this work can be used as a metrological tool for estimating the

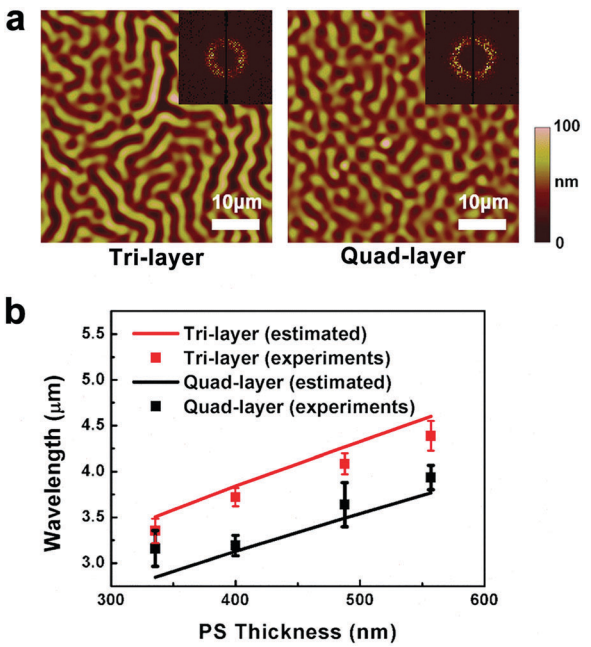

Fig. 3 Different surface wrinkling according to the number of multilayers. (a) AFM images of wrinkled surfaces of tri-layer and quad-layer systems. For both samples, the thickness of the underlying PS is 490 nm, and the total thickness of the capping layer (Al and P4VP) is 40 nm. (b) Comparison between theoretical (solid lines) and experimental (square dots) results. Wrinkles from the quad-layer systems (black) show smaller wavelengths than those from tri-layer systems (red).

thermomechanical properties of a polymer. Although wrinkling-based metrology, representatively termed "strain-induced elastic buckling instability for mechanical measurements (SIEBIMM)", has been well developed since a pioneering work reported by Stafford *et al.*, previous work has been primarily designed to estimate the modulus of a rigid elastic layer that is thermally insensitive.[49] However, a polymer's thermomechanical response, by which the Young's modulus varies over a broad range by temperature, indicates that thermally sensitive polymeric systems are not readily applicable to SIEBIMM. On the other hand, as shown in this study, a targeted polymeric layer can be incorporated into the capping layer, and the results of thermal wrinkling can be expressed using the collective contributions of each constituent layer. Therefore, the thermomechanical properties of a polymer can be precisely estimated with respect to temperature variations.

Using this strategy, we investigated a polymer's variation in Young's modulus near the T_g region. As shown in the schematic drawing in Fig. 4a, tri-layer samples with PS (490 nm)/Al (13 nm)/P4VP (60 nm) were prepared and subjected to thermal annealing (12 h) between 132 and 156 °C. We then back-calculated the observed wrinkling wavelength using eqn (2) to obtain the Young's modulus of the uppermost P4VP layer. The experimentally estimated Young's moduli of the thin P4VP layer in response to temperature variations are presented in Fig. 4b. The bulk-phase modulus of P4VP (4 GPa) decreased rapidly in the vicinity of its T_g (148 °C, obtained from ellipsometric measurements), and the rubbery-phase modulus eventually weakened to several MPa above 156 °C. To validate this trend using a known relation, we used the WLF equation. The calculated results are drawn in Fig. 4b as a solid black curve. For this system, we used T_r = 421 K, C_1 = 17.4, C_2 = 51.6 K, and $E_{P4VP,0}$ = 4 GPa.[39,40] In contrast, the WLF equation presents a precipitous drop in Young's modulus near T_g due to the restriction imposed by the mathematical expression, as shown in eqn (3), the experimentally estimated values obtained using the suggested metrology predict a subtle change in the moduli even in the GPa order, imparting the capability of high precision measurement of the thermomechanical properties of polymers.

Thermal wrinkling-based metrology for investigating the elastic properties of polymers has been previously studied using the polymeric layer as the underlying substrate and an applied temperature much higher than T_g of the polymer to induce thermal wrinkling.[50] However, the approach presented here includes the targeted polymer in the capping layer, which allows the monitoring of delicate changes in its elastic properties near its T_g through wavelength changes in surface wrinkling. Therefore, this method could be widely used to estimate T_g of unknown polymers and to obviate the use of complicated optical or thermomechanical characterization facilities.

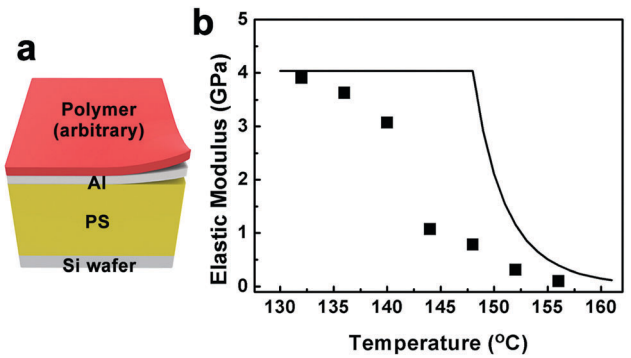

Fig. 4 (a) Schematic illustration of tri-layer wrinkling to estimate the thermomechanical properties of the uppermost polymeric layer. (b) Estimated elastic moduli (marked in black square dots) of a 60 nm-thick layer of P4VP between 132 and 156 °C. The solid line represents the varying trend of Young's modulus according to the WLF equation.

Conclusions

In this work, we suggested a cumulative energy analysis to interpret thermally induced wrinkling for heterogeneous multilayer systems. The energetic contribution of the bending deformation of the capping layer comprising metal/polymer multilayers is individually considered for each constituent layer. The resulting estimated wavelength matches well with the experimental data for tri- and quad-layer systems. Compared with the composite layer model, in which the bending energy of a combined single capping layer is highly overestimated, the individual layer model and cumulative energy analysis enable accurate interpretation of the wrinkling energies. Also, the multilayer wrinkling approach can be used to design and generate smaller wrinkles for specific applications. Finally, the proposed method is an efficient metrological tool for estimating the thermomechanical properties of polymers near their T_g, which are otherwise difficult to obtain. Therefore, this work will be highly beneficial for elucidating multilayer wrinkling phenomena and creating optically responsive novel surface structures.

Conflicts of interest

There are no conflicts to declare.

Acknowledgements

This work was supported by the Samsung Research Funding Center for Samsung Electronics under Project Number SRFC-MA1402-09.

Notes and references

1 N. Bowden, S. Brittain, A. G. Evans, J. W. Hutchinson and G. M. Whitesides, *Nature*, 1998, **393**, 146–149.
2 P. C. Lin, S. Vajpayee, A. Jagota, C. Y. Hui and S. Yang, *Soft Matter*, 2008, **4**, 1830–1835.
3 P. C. Lin and S. Yang, *Soft Matter*, 2009, **5**, 1011–1018.
4 J. Yang, S. Damle, S. Maiti and S. S. Velankar, *Soft Matter*, 2017, **13**, 776–787.

5 P. J. Yoo, S. Y. Park, S. J. Kwon, K. Y. Suh and H. H. Lee, *Appl. Phys. Lett.*, 2003, **83**, 4444–4446.
6 D. B. H. Chua, H. T. Ng and S. F. Y. Li, *Appl. Phys. Lett.*, 2000, **76**, 721–723.
7 M. Guvendiren, S. Yang and J. A. Burdick, *Adv. Funct. Mater.*, 2009, **19**, 3038–3045.
8 Z. Wu, N. Bouklas and R. Huang, *Electron. Mater. Lett.*, 2013, **50**, 578–587.
9 P. J. Yoo and H. H. Lee, *Langmuir*, 2008, **24**, 6897–6902.
10 B. A. Glatz, M. Tebbe, B. Kaoui, R. Aichele, C. Kuttner, A. E. Schedl, H. W. Schmidt, W. Zimmermann and A. Fery, *Soft Matter*, 2015, **11**, 3332–3339.
11 S. E. Song, G. H. Choi, G. R. Yi and P. J. Yoo, *Soft Matter*, 2017, **13**, 7753–7759.
12 J. Y. Chung, A. J. Nolte and C. M. Stafford, *Adv. Mater.*, 2011, **23**, 349–368.
13 L. Zhu and X. Chen, *J. Eng. Mater. Technol.*, 2017, **139**, 021021.
14 D. Tahk, H. H. Lee and D. Y. Khang, *Macromolecules*, 2009, **42**, 7079–7083.
15 D. J. Lipomi, H. Chong, M. Vosgueritchian, J. Mei and Z. Bao, *Sol. Energy Mater. Sol. Cells*, 2012, **107**, 355–365.
16 J. Hou, Q. Li, X. Han and C. Lu, *J. Phys. Chem. B*, 2014, **118**, 14502–14509.
17 F. A. Bayley, J. L. Liao, P. N. Stavrinou, A. Chiche and J. T. Cabral, *Soft Matter*, 2014, **10**, 1155–1166.
18 J. Y. Park, H. Y. Chae, C. H. Chung, S. J. Sim, J. Park, H. H. Lee and P. J. Yoo, *Soft Matter*, 2010, **6**, 677–684.
19 Y. Liu, M. Li, J. Liu and X. Chen, *J. Appl. Mech.*, 2017, **84**, 051011.
20 P. J. Yoo and H. H. Lee, *Phys. Rev. Lett.*, 2003, **91**, 154502.
21 R. Huang, *J. Mech. Phys. Solids*, 2005, **53**, 63–89.
22 M. D. Casper, A. Ö. Gözen, M. D. Dickey, J. Genzer and J. P. Maria, *Soft Matter*, 2013, **9**, 7797–7803.
23 F. Wang, Z. Wang, C. Jiang, L. Yin, R. Cheng, X. Zhan, K. Xu, F. Wang, Y. Zhang and J. He, *Small*, 2017, **13**, 1604298.
24 X. Chen and J. W. Hutchinson, *J. Appl. Mech.*, 2004, **71**, 597–603.
25 J. Zhao, X. Guo and L. Lu, *J. Appl. Math. Mech. (Engl. Transl.)*, 2017, **38**, 617–624.
26 A. L. Volynskii, O. V. Lebedeva, N. F. Bakeev and S. Bazhenov, *J. Mater. Sci.*, 2000, **35**, 547–554.
27 C. Zong, Y. Zhao, H. Ji, J. Xie, X. Han, J. Wang, Y. Cao, C. Lu, H. Li and S. Jiang, *Macromol. Rapid Commun.*, 2016, **37**, 1288–1294.
28 E. Lejeune, A. Javili and C. Linder, *Soft Matter*, 2016, **12**, 806–816.
29 A. R. Shugurov, A. L. Kozelaskaya and A. V. Panin, *RSC Adv.*, 2014, **4**, 7389–7395.
30 E. Cerda and L. Mahadevan, *Phys. Rev. Lett.*, 2003, **90**, 074302.
31 S. J. Kwon, J. H. Park and J. G. Park, *Phys. Rev. E: Stat., Nonlinear, Soft Matter Phys.*, 2005, **71**, 011604.
32 P. J. Yoo, K. Y. Suh, S. Y. Park and H. H. Lee, *Adv. Mater.*, 2002, **14**, 1383–1387.
33 P. J. Yoo and H. H. Lee, *Macromolecules*, 2005, **38**, 2820–2831.
34 P. J. Yoo, *Electron. Mater. Lett.*, 2011, **7**, 17–23.
35 L. D. Landau and E. M. Lifshitz, *Theory of Elasticity*, Pergamon, NY, 3rd edn, 1986.
36 J. Groenewold, *Physica A*, 2001, **298**, 32–45.
37 P. J. Yoo, K. Y. Suh, H. Kang and H. H. Lee, *Phys. Rev. Lett.*, 2004, **93**, 034301.
38 A. J. Nolte, R. E. Cohen and M. F. Rubner, *Macromolecules*, 2006, **39**, 4841–4847.
39 T. Dequivre, E. Al Alam, J. Plathier, A. Ruediger, G. Brisard and S. A. Charlebois, *ECS Trans.*, 2015, **69**, 91–97.
40 M. L. Williams, R. F. Landel and J. D. Ferry, *J. Am. Chem. Soc.*, 1955, **77**, 3701–3707.
41 E. P. Chan, S. Kundu, Q. Lin and C. M. Stafford, *ACS Appl. Mater. Interfaces*, 2011, **3**, 331–338.
42 J. S. Sharp and J. A. Forrest, *Phys. Rev. Lett.*, 2003, **91**, 235701.
43 C. M. Stafford, B. D. Vogt, C. Harrison, D. Julthongpiput and R. Huang, *Macromolecules*, 2006, **39**, 5095–5099.
44 Y. H. Park, N. A. Kumar, J. Y. Kim, J. T. Kim, K. T. Lim and Y. T. Jeong, *Eur. Polym. J.*, 2007, **43**, 5034–5039.
45 C. A. Tweedie, G. Constantinides, K. E. Lehman, D. J. Brill, G. S. Blackman and K. J. Van Vliet, *Adv. Mater.*, 2007, **19**, 2540–2546.
46 C. M. Stafford, S. Guo, C. Harrison and M. Y. M. Chiang, *Rev. Sci. Instrum.*, 2005, **76**, 062207.
47 J. H. Na, S. U. Kim, Y. Sohn and S. D. Lee, *Soft Matter*, 2015, **11**, 4788–4792.
48 A. Balčytis, M. Ryu, G. Seniutinas, P. R. Stoddart, M. A. Al Mamun, J. Morikawa and S. Juodkazis, *Nanoscale*, 2017, **9**, 690–695.
49 C. M. Stafford, C. Harrison, K. L. Beers, A. Karim, E. J. Amis, M. R. Vanlandingham, H. C. Kim, W. Volksen, R. D. Miller and E. E. Simonyi, *Nat. Mater.*, 2004, **3**, 545–550.
50 E. P. Chan, K. A. Page, S. H. Im, D. L. Patton, R. Huang and C. M. Stafford, *Soft Matter*, 2009, **5**, 4638–4641.

